EXPERIMENTAL INVESTIGATION ON TRANSIENT HEAT TRANSFER CHARACTERISTICS OF C-SHAPE HEATING ROD BUNDLE USED IN PRHR HX

ZHANG Yuhao, LU Daogang, and WU Guanghao
School of Nuclear Science and Engineering, North China Electric Power University
No.2, Beinong Road, Changping, Beijing 102206, China
Beijing Key Laboratory of Passive Safety Technology for Nuclear Energy, North China Electric Power University, Beijing 102206, China
zyhncepu@163.com; ludaogang@ncepu.edu.cn; special630@163.com

DU Zheng
State Nuclear Power Software Development Center
Beiqijia Road, Changping, Beijing 100029, China
duzheng@snptc.com.cn

ABSTRACT

The heat transfer capacity of Passive Residual Heat Removal Heat Exchanger (PRHR HX) and thermal stratification in the In-containment Refueling Water Storage Tank (IRWST) are of great importance for the efficient and safe removal of the residual heat in the AP1000 reactor. The C-type heating rods bundle is being used in the PRHR HX, yet the heat transfer characteristics of this special shape heat exchanger are not completely explicit. In the present work, an overall scaled IRWST (irregular shaped tank, approximate 4m×1.5m×2.5m) and PRHR HX models were built to simulate the thermal-hydraulic process in the residual heat removal accident, which was the first overall scaled separate effect IRWST&PRHR HX experiment compared to the previous work. More than 150 T-type thermocouples were utilized to measure the temperature, and the Particle Image Velocimetry (PIV) were utilized for the measurement of the flow velocity. Based on the experimental data, the transient heat transfer characteristics of C-shaped heating rod bundle were analyzed. Combination factors including the flow resistance, buoyancy-induced flow velocity, and turbulent mixing effects imposed important impacts on the heat transfer capability of the PRHR HX model. The Nu variations trend indicated that the experimental data were in satisfactory agreement with the empirical correlations in the single convection stage, and the heat transfer capability in the vertical section was better.

KEYWORDS
C-shaped heating rod bundle, PRHR HX, transient heat transfer characteristics, IRWST

1. INTRODUCTION

In advanced passive pressurized water reactor (PWR) design, passive safety systems are widely implemented. Typically, the large special-shape tank, In-containment Refueling Water Storage Tank (IRWST), has been applied in the Generation III advanced nuclear power plant AP1000. The C-shape Passive Residual Heat Removal Heat Exchanger (PRHR HX) immerged in the IRWST is a critical component in the Passive Residual Heat Removal System (PRHRS). The PRHR HX connects through the inlet and outlet lines to Reactor Coolant System (RCS) loop 1 and locates above RCS loops. During the Station Blackout (SBO) accident or the Loss of Coolant Accident (LOCA), the PRHR will be actuated by density contrast between PRHR HX and RCS loop [1]. As a result, the core decay heat is removed continuously by natural circulation and transferred to the IRWST via the PRHR HX.

In the aspect of previous experimental research, the Westinghouse Electric Corporation has performed PRHR HX separate effect experiment [2] for AP600, utilizing 3 vertical tubes to validate the heat transfer capability of the PRHR HX. However, the horizontal sections of PRHR HX were neglected, and a simplified vertical cylinder pool was utilized to simulate the IRWST, which was different with the prototype. In the actual design of the AP1000 reactor, the horizontal sections of the PRHR HX were further elongated. As a result, the impact of the horizontal sections should be taken into consideration in the experiment. In addition, although some integral effect experiments such as APEX [3, 4], ROSA [5] etc. involved PRHR HX model equipment, attentions were mainly concentrated on the integral system functions, rather than the local heat transfer effects. Besides, Moon-Hyun Chun [6] studied the effects of the heat exchanger tube geometries on heat transfer in a scaled tank using 3 straight heating rods. Various combinations of tube diameters, surface roughness, and tube orientation were discussed. Li [7] performed experiment on the heat transfer effect of vertical tube bundle immerged in an elevated tank during the initial operation stage of the PRHR HX. Gandhi [8], Ganguli [9]conducted single heating tube experiment, and utilized CFD simulation to investigate the extent of stratification, the velocity distribution, and the turbulent parameters, etc.

According to the previous investigations, attentions were mainly focused on the heat transfer mechanism of horizontal or the vertical bundle separately. Moreover, the dimension of the prototype equipment was too large and the IRWST was also in irregular shape, it was almost impossible to conduct the full-scale experimental research. In the present work, the transient heat transfer characteristics of the C-shape rod bundle model used in PRHR HX were investigated based on an overall scaled IRWST&PRHR HX test bench. The transient heat transfer characteristics of the PRHR HX as well as IRWST were investigated.

2. EXPERIMENTAL SET-UP

The prototype of IRWST was irregular shape tank with PRHR HX located at one side of the tank, which was shown in Fig. 1.

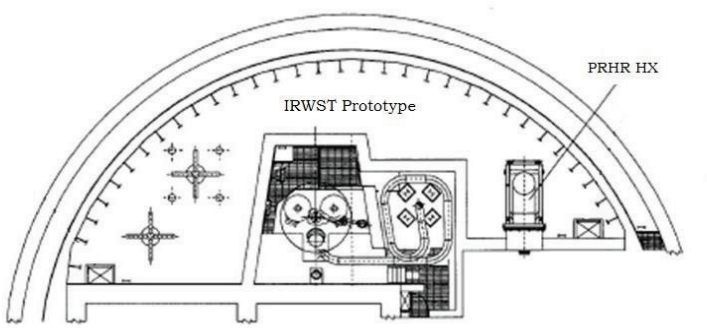

Figure 1. Shape of IRWST and Location of PRHR HX.

Performing experiments investigation in an actual scale of the equipment is impractical owing to the realizability and cost limitations, and even impossible for the enormous dimensions of the prototype in the reactor. In such case, the overall scaled-down separate-effects IRWST&PRHR HX experimental model was conducted to simulate the thermal-hydraulic phenomena in the accidental events based on the scaling criterions.

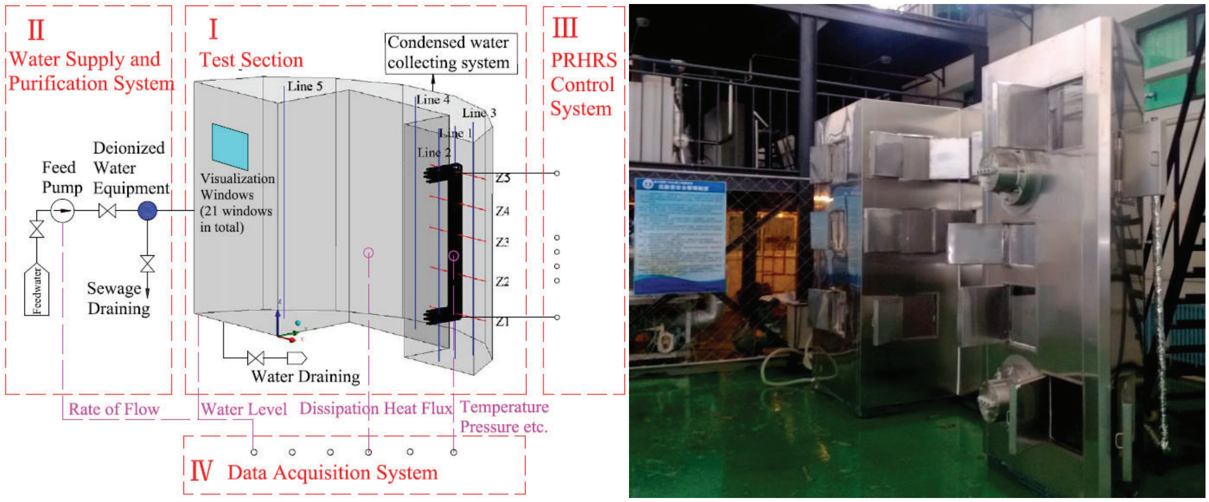

(a)Arrangement of Experimental Setup. (b) Schematic of Actual Experimental Facilities.

Figure 2. Schematic of Experimental Setup.

A schematic of the experimental setup was shown in Fig. 2(a). It consisted of four major systems including I. Test section, II. Water supply and purification system, III. PRHR control system, IV. Data acquisition system. The test section mainly contained PRHR HX model, IRWST model, as well as auxiliary equipment.

In the actual working condition of AP1000 nuclear power plant, hot coolant of 570.35K flows into the inlet of PRHR HX and cools down along the 689 tubes C-shape bundle, so the thermal power decreases along the flow direction, resulting in the non-uniform heat flux. In the present work, more attentions were focused on the effects of the special C-shape as well as the secondary heat transfer characteristics in IRWST, so the heat transfer capability was evaluated in the averaged uniform heat flux. Based on this purpose, simplifications were implemented on the PRHR HX model wall heat flux. The PRHR HX was simulated by 12 symmetrically arranged C-shape electrical heating rods bundle, and a simplified averaged heat flux of $120000W/m^2$ was set on the PRHR HX model wall, which was the same to the averaged heat flux along the prototype PRHR HX. Then the proportionally scaled down power of 176kW was thus obtained. The IRWST model was scaled down to approximately 4m×1.5m×2.5m with a wall thickness of 8mm using 304 stainless steel, and the normal water level was set as 2.2m. The PRHR HX model was arranged on one side of the tank and the special shape of IRWST model was similar to the prototype.

Table I. Comparison of the parameters between prototype and experimental model

Items	Prototype	Scaled model
Scale ratio in length	1	About 1/11.3
Scale ratio in height	1	About 1/4
Initial water temperature in IRWST	322.05K	322.05K
PRHR HX tubes number	689	12
Outside diameter of heat transfer tube	19mm	19mm
Distance between heat transfer tubes	38mm	38mm
Heat power	5.89×10^7W	About 176 kW

Total of 21 visualization windows were set on selected locations of the IRWST model wall. Then the PIV (TSI INSIGHT) were utilized for the measurement of the 2-D single flow velocity. In addition, the 50mm thick insulating layers made by aluminum silicate wool were pasted on the outside surface of the IRWST model walls. The comparison of the key parameters between the prototype and the experimental model were listed in Table I.

For the temperature measurement, more than 150 T-type calibrated thermocouples (stainless steel sheathed) were utilized to monitor the transient temperature variations in the key regions including the walls of heating rods, the channels within the rods bundle, and the around bulk fluid region. Thermocouples as thin as 0.5mm in diameter were used, and the locations of the thermocouples were precisely distributed along the thin stainless wires, to ensure that the influences on the flow patterns to be minimized. Moreover, the end of the thermocouples was carefully spot welded on the heating rods walls in different flow channels to get the wall temperature.

PIV technique was utilized to measure the local buoyancy-induced velocity in the central plane of the bundle region. The measuring strategies including the arrangement of the laser transmitter, CCD camera, and the monitoring plane were schematically shown in Fig. 3.

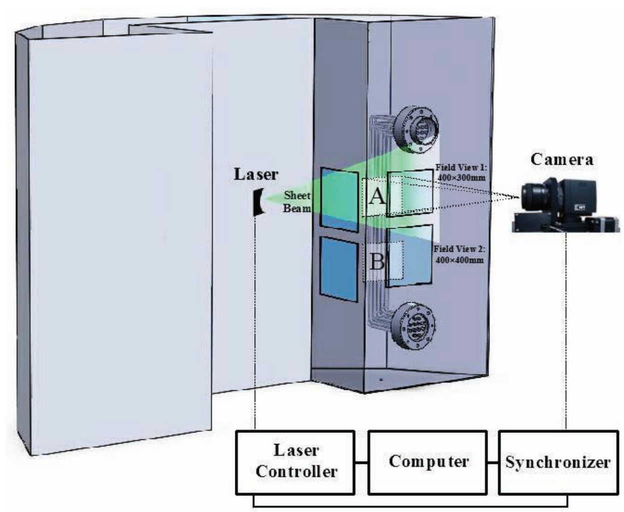

Figure 3. Arrangement of the PIV Components.

Auxiliary parameters including feed water flow rate, water level, pressure etc. were also monitored. All sensors were connected to six 32-channenel input modules (NI PXIe-4353) and analyzed by the Data Acquisition System (NI PXIe-8115) with the data-sampling rate of 5Hz.

3. OVRALL THERMAL-HYDRAULICS PARAMETER ANALYSIS

The locations of the monitoring lines were shown in Fig. 4(a), and moreover, the normalized dimensionless coordinates were employed and defined by $x^* = x / X$, which was also applicable to Y and Z coordinates. The top view of the positions of monitoring lines in the normalized coordinate axis was schematically shown in Fig. 4(b).

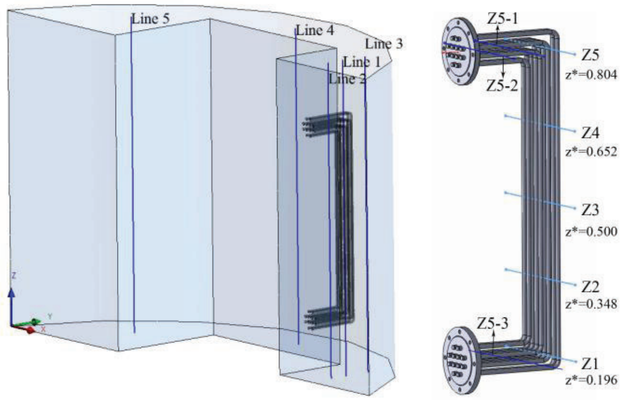

(a) Locations of the Monitoring Lines.

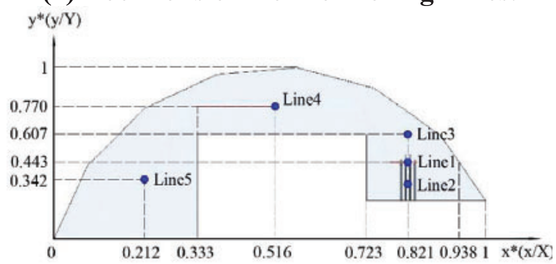

(b)Dimensionless Locations of the Monitoring Lines.

Figure 4. Locations of the Monitoring Lines.

The temperature distributions at typical moments along Line 1, 2, 3, 5 were shown in Fig. 4. According to the monitored temperature lines at 500s, when the fluid was heated by the C-shape PRHR HX model, buoyancy-induced water flowed up and changed directions, eventually leading to the natural convection in the IRWST within a relatively short time. The phenomenon of thermal stratification in the IRWST was obvious, and temperature was apparently higher within the C-shape tubes bundle region (Line 1). Moreover, as shown in Line 2, the existence of C-shape bundle led to special temperature trends. Two temperature peaks appeared when it passed through both the upper and lower horizontal rod bundles regions. The temperature along Line 3 and 5 showed similar trend, and it meant that the natural convection has already built, and the heated fluid flowed to the other side of IRWST in relative short time.

As time proceeded, Fig. 5(b) indicated that the thermal stratification along the height direction became more evident, whereas the temperature difference along the lateral direction was smaller at 3000s. It could be explained as follows. With the increasing of heating time, the natural convection was enhanced, and the flowing of the fluid resulted in uniform temperature distributions along the lateral direction. However, the buoyance-induced density differences prevented the mixing effect in the height direction.

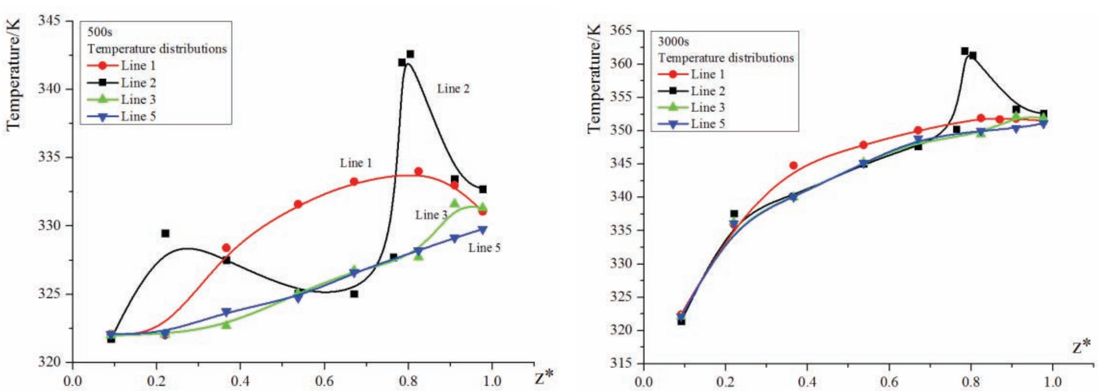

(a)Temperature Distributions at 500s. (b) Temperature Distributions at 3000s.
Figure 5. Temperature Distributions in the height direction.

The transient variations of temperature of center points at different heights along Line 1 were recorded as Fig. 6. It indicated that the local temperature increased continuously until it reached 373.15K. Moreover, temperature differences were also obvious in the center vertical sections of PRHR HX bundle. It tool approximate 7000s, i.e. 2h for the fluid to reach the boiling point in the center of PRHR HX bundle.

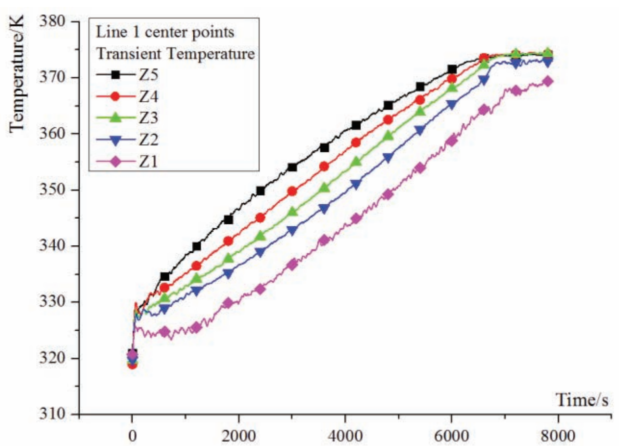

Figure 6. Transient Temperature of Center Points along Line 1.

The velocity field was generated by the temperature differences, and in turn, it affected the temperature distributions. PIV (TSI INSIGHT) technique was employed to measure the local flow velocity in the vertical bundle region of the PRHR HX between Z3 and Z4 shown in Fig. 4(a). The PIV captured PRHR HX bundle region was schematically shown in Fig. 7(a), and the corresponding captured velocity distributions were shown in Fig. 7(b).

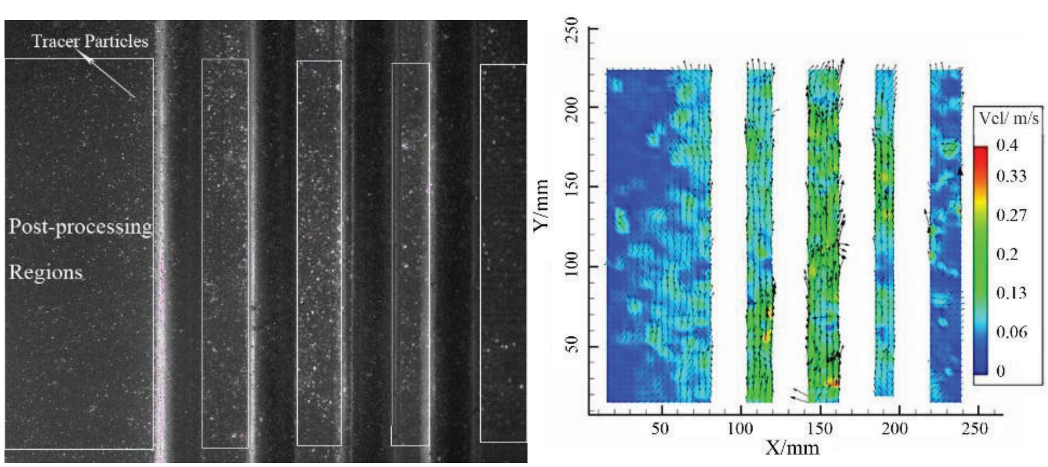

(a) PIV Captured Actual PRHR HX Bundle Region (b) PIV Captured Velocity Distributions
Figure 7. PIV Captured Results

In the PIV experimental results, only the sub-channels between the 4 tubes could be captured, as the existence of the tubes in the front would cover the fluid channels. Moreover, the captured results were sensitive to external factors including the laser intensity, focused effect, etc. Considering the mentioned factors and capture effect, the 250×220mm scope were selected for post-processing (Fig. 7(b)). The PIV results indicated that the majority of fluid flowed upward within the bundle region. The maximum velocity values were approximately 0.2m/s. Besides, the velocity outside the C-shape bundle region decreased significantly, as the fluid moved toward the radial direction and developed the overall natural circulation in the tank.

4. HEAT TRANSFER ANALYSIS

The variations of averaged heat transfer coefficient (HTC) along the C-shape bundle were shown in Fig. 8. The locations of the monitoring points were shown in Fig. 4. According to the variations of HTC, in the initial stage of 3000s, the single phase natural convection takes the dominant role, so the heat transfer effect is slightly enhanced and the heat transfer coefficient increases little during this stage. Then the nucleate boiling begins, and the generation, separation, and buoyancy-lift of the bubbles enhance the heat transfer effect significantly. As a result, the HTC increased rapidly after 5000s. In the aspect of the vertical bundle region, the HTC increases along the height direction, and the HTC peak values appear in the upper vertical region. And in two phase flow region, the flowing up bubbles also enhance the mixing effects, and this effects become more and more evident in the upper region of the vertical bundle, leading to the abrupt increase of the HTC in this region.

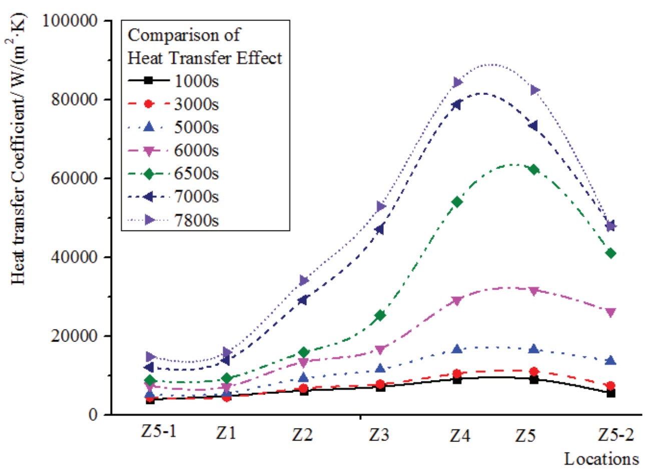

Figure 8. Variations of HTC at Different Time

As discussed above, the transient heat transfer characteristics of the C-shape PRHR HX bundle were influenced by complicated factors, and Nusselt number (Nu) reflected the heat transfer effects of the heating rod bundle, then the transient variations of mean Nu were analyzed as follows. Correlations for Nu of both horizontal and vertical cylinders in single natural convection stage were employed to compare with the experimental data.

For horizontal cylinder, the Nu correlation proposed by Churchill and Chu [10] was defined as:

$$Nu = \left\{ 0.60 + \frac{0.387 Ra^{1/6}}{\left[1 + (0.559/\Pr)^{9/16}\right]^{8/27}} \right\}^2 \tag{1}$$

Eq. 1 has a wide application scope of Ra<10^{13}.

Furthermore, in the initial single phase flow stage, the flow pattern for free convection in the horizontal bundle region changed from laminar to turbulent gradually, and another correlation for laminar flow from a horizontal cylinder with a uniform heat flux density obtained by Churchill [11] was defined as:

$$Nu = 0.579 \left(\frac{Ra}{\left[1 + \left(0.442/\Pr\right)^{9/16}\right]^{16/9}} \right)^{1/4} \tag{2}$$

In the present work, the uniform heating condition was applied on the walls of the PRHR HX model. In order to avoid the explicit inclusion of temperature differences, the correlations were rewritten in terms of Ra*. Further, Churchill and Chu [10] pointed out that the dependence of Nu on Ra was essentially the same for uniform heat flux as for uniform wall temperature. So the Ra* and Gr* were revised as:

$$Ra^* = Gr^* \cdot \Pr \tag{3}$$

$$Gr^* = \frac{g \beta q D_e^4}{\lambda \nu^2} \tag{4}$$

In the aspect of vertical bundle, the Nu was recommended as: [12]

$$Nu = \left\{ 0.825 + \frac{0.387 Ra^{1/6}}{\left[1 + (0.492/\Pr)^{9/16}\right]^{8/27}} \right\}^2 \tag{5}$$

In the horizontal sections shown in Fig. 9, the velocity of the buoyancy-induced flow was so slow that the flow pattern was kept in laminar in the initial stage of the heating process. As time proceeded, the velocity increased and the existence of the rods bundle enhanced the mixture effects between the flow channels, leading to the increase of the Nu values.

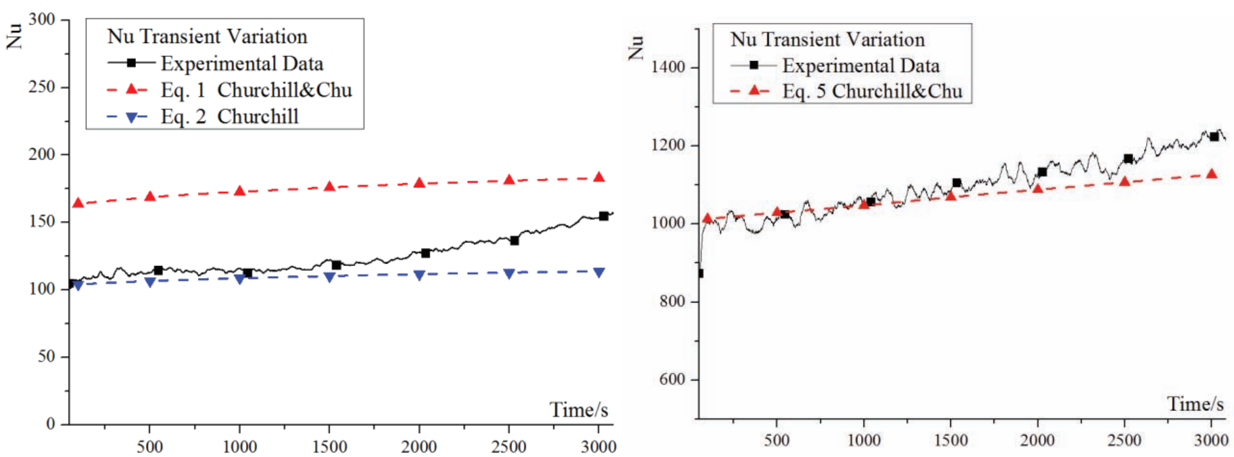

Figure 9. Nu Comparison in Horizontal Section. **Figure 10. Nu Comparison in Vertical Section.**

Fig. 10 quantitatively showed the transient variations of the mean Nu in the vertical bundle along the monitoring line of Z 4 (shown in Fig. 4). In this section, with the heated fluid in the lower section flowing up in relatively high velocity with little resistance, the heat transfer effect was apparently better, and the experimental Nu valves were in satisfactory agreement with the Eq. 5 predicted values in the initial 2000s. Then the experimental Nu increased with the enhancement of the turbulent mixture effects in the bundle region compared to the Eq. 5. And after approximate 3000s, two phase boiling stage began, and the heat transfer effect was further enhanced.

According to the comparison between horizontal and vertical sections, the measured Nu values in the vertical bundle were approximately 8-10 times higher than those in the horizontal bundle. It revealed that the heat transfer capability in the vertical section was better due to the combination factors including the lower flow resistance, higher buoyancy-induced flow velocity, and enhanced turbulent mixing effects. When the nucleate boiling began, the selected single natural convection correlations were no more appropriate, and the boiling empirical correlations would be analyzed in the next step.

5. CONCLUSIONS

In the present work, the transient heat transfer characteristics of the C-shape rod bundle model used in PRHR HX were investigated based on an overall scaled IRWST&PRHR HX test bench. The transient heat transfer characteristics of the PRHR HX as well as IRWST were investigated. The main conclusions were as follows.

(1) The PRHR HX residual heat was removed to the IRWST continuously and steadily by natural convection, and thermal stratification occurred in the overall tank. It took approximate 7000s for the fluid to reach the boiling point in the surface of the water.

(2) The transient thermal hydraulics analysis indicated that the natural convection was caused by temperature difference, and the velocity field was generated by the temperature field, and in turn, affected the temperature field.

(3) Combination factors including the flow resistance, buoyancy-induced flow velocity, and turbulent mixing effects imposed important impacts on the heat transfer capability of the PRHR HX model. The analysis of the Nu number variations indicated that the experimental data were in satisfactory agreement with the empirical correlations in the single convection stage.

(4) Nu values in the vertical bundle were approximately 8-10 times higher than those in the horizontal bundle. It revealed that the heat transfer capability in the vertical section was better due to the combination factors.

NOMENCLATURE

g	gravitational acceleration (m/s^2)
Gr	Grashof number(−)
k	turbulence kinetic energy (J/kg)
Nu	Nusselt number(−)
Pr	Prandtl number(−)
q	heat flux (W/m^2)

Ra	Rayleigh number(−)
Re	Reynolds number(−)
T	temperature (K)
x	any distance along the length of IRWST model tank (m)
x^*	normalized length(−)
X	total length of IRWST model tank (m)
y	any distance along the width of IRWST model tank (m)
y^*	normalized width(−)
Y	total width of IRWST model tank (m)
z^*	normalized height(−)

Greek symbols

β	thermal expansion coefficient (K^{-1})
λ	thermal conductivity (W/(m·K))
ρ	density of fluid (kg/m^3)
μ	dynamic viscosity ($N\cdot s/m^2$)
ν	kinematic viscosity (m^2/s)

Subscripts

i, j	tensor
t	turbulent

Abbreviation

CCD	charge coupled device
IRWST	In-containment Refueling Water Storage Tank
PIV	Particle Image Velocimetry
PRHR HX	Passive Residual Heat Removal Heat Exchanger
SBO	Station BlackOut accident

ACKNOWLEDGMENTS

Thanks for the sponsoring of National Science and Technology Major Project, China. (2011ZX06004-024-07-03-00), Beijing Key Laboratory of Passive Safety Technology for Nuclear Energy and Chinese Universities Scientific Fund, and Combined training joint project for graduate student in Beijing.

REFERENCES

1. Lin, C. and Z. Yu, *The Advanced Passive Pressurized Water Reactor AP1000*, pp. 438-450, Atomic Energy Press, Beijing, China (2008).
2. Hochreiter, L.E., F.E. Peters, and D.L. Paulsen, "*AP600 Passive Residual Heat Removal Heat Exchanger Test Final Report,"* USA (1997).
3. Jr, J.N.R. and L. Hochreiter, "Scaling analysis for the OSU AP600 test facility (APEX)," *Nuclear Engineering and Design.* **186**, pp. 53-109.
4. Reyes, J.N., et al., "Final Report for the OSU APEX-CE Integral System Test Facility Test Results," Nuclear Regulatory Commission, USA (2004)
5. Takeda, T., H. Asaka, and H. Nakamura, "Analysis of the OECD/NEA ROSA Project experiment simulating a PWR small break LOCA with high-power natural circulation," *Annals of Nuclear Energy*. **36**(3): p. 386-392 (2009)

6. Chun, M.H. and M.G. Kang, “Effects of heat exchanger tube geometries on nucleate pool boiling heat transfer in a scaled In-containment Refueling Water Storage Tank,” *International communications in Heat and Mass Transfer*. **23**(1), pp. 23-34 (1996).
7. Li, Y., et al., “Research on Heat Transfer Characteristic of PRHR HX at Initial Operating Stage,” *Atomic Energy Science and Technology*. **45**(8), pp. 931-936 (2011).
8. Gandhi, M.S., et al., “Reduction in thermal stratification in two phase natural convection in rectangular tanks: CFD simulations and PIV measurements,” *Chemical Engineering Science*. **100**, pp. 300-325 (2011).
9. Ganguli, A.A., et al., “Hydrodynamics and heat transfer characteristics of passive decay heat removal systems: CFD simulations and experimental measurements,” *Chemical Engineering Science*. **65**(11), pp. 3457-3473 (2010).
10. Chruchill, S.W. and H.H.S. Chu, “Correlating equations for laminar and turbulent free convection from a horizontal cylinder,” *International Journal of Heat and Mass Transfer*. **18**, pp. 1049-1053 (1975).
11. Churchill, S.W., “Laminar free convection from a horizontal cylinder with a uniform heat fulux density,” *Letters in Heat and Mass Transfer*. **1**, p. 109-112 (1974).
12. Churchill, S.W. and H.H.S. Chu, “Correlating equations for laminar and turbulent free convection from a vertical plate,” *International Journal of Heat and Mass Transfer*. **18**(11): p. 1323-1329 (1975).